Applied Physics A (2020) 126:165
https://doi.org/10.1007/s00339-020-3347-5

Applied Physics A
Materials Science & Processing

Inline monitoring of hydrogenous plasma-induced defect formation within fused silica via plasma emission spectroscopy

Christoph Gerhard[1] · Emilie Letien[2] · Thomas Cressent[3] · Mandy Hofmann[4]

Received: 15 November 2019 / Accepted: 27 January 2020
© The Author(s) 2020

Abstract
In this paper, the indirect monitoring of plasma-induced defect formation within fused silica via plasma emission spectroscopy is presented. It is shown that low-pressure plasma treatment with hydrogen as process gas leads to a decrease in UV transmission of fused silica. This decrease can be directly attributed to oxygen vacancy-related defects and the presence of hydrogen within the silicon dioxide glass network. By the analysis of the plasma composition, it was observed that the amount of oxygen within the plasma increases with increasing treatment duration. Hence, oxygen was continuously released from glass network in the course of the plasma treatment. It was further observed that this release is strongly dependent on the applied plasma power where the lowest process efficiency occurs at the highest plasma power. It is shown that an increase in plasma power leads to a remarkable increase in light emission from the working gas, hydrogen. This observation indicates that the higher the degree of excitation and ionisation of the plasma, the lower the efficiency of plasma-induced formation of oxygen deficiency-related defects. This finding is of mentionable relevance for a better understanding of plasma-induced surface modification and coating processes.

Keywords Fused silica · Optical properties · Oxygen deficiency · Glass defects · Plasma treatment · Plasma emission spectroscopy

1 Introduction

In the last decades, the understanding of oxygen deficiency centres (ODC), hydrogen centres and other oxygen deficiency-related defects such as E′-centres in glasses has gained in importance due to the growing number of optical and opto-electrical devices and systems used in telecommunication, medical technology, laser-based manufacturing, etc. It is well known that oxygen deficiency leads to intrinsic point defects in glasses [1] that may decrease transmission—a mechanism which is of essential relevance in optical fibres and fibre networks [2]. In addition to an increase in absorption in the ultraviolet wavelength range [3], the presence of oxygen deficiency centres can also give rise to disturbing (and partially long-term) phosphorescence after irradiation by any light source [4]. Against this background, the actual formation as well as the prediction of oxygen deficiencies via modelling was investigated intensively in the past [5].

However, in contrast to the above-mentioned disturbing and unwanted effects, an oxygen deficiency-related increase in absorption is of certain interest for laser structuring of optical glasses and particularly fused silica [6–8]. It was shown in previous work that for this purpose, oxygen deficiency centres and the accompanying increase in absorption can be generated selectively by plasma-induced chemical reduction of glass-forming oxides [9, 10]. Hence, the dependency of a plasma-induced decrease in transmission of fused silica and the accompanying enrichment of the

✉ Christoph Gerhard
christoph.gerhard@hawk.de

[1] Fakultät Naturwissenschaften und Technik, Hochschule für Angewandte Wissenschaft und Kunst, Von-Ossietzky-Straße 99, 37085 Göttingen, Germany

[2] Département Mesures Physiques, Institut Universitaire de Technologie A de Lille, Avenue Paul Langevin – Cité scientifique, BP 90179, 59653 Villeneuve d'Ascq Cedex, France

[3] Département Chimie, Institut Universitaire de Technologie A de Lille, Le Recueil – Rue de la recherche, BP 90179, 59653 Villeneuve d'Ascq Cedex, France

[4] Fachbereich Ingenieur- und Naturwissenschaften, Technische Hochschule Wildau, Hochschulring 1, 15745 Wildau, Germany

Published online: 07 February 2020

plasma volume with oxygen from the silicon dioxide glass matrix on the plasma power and treatment duration were investigated in the present work. One has to consider that the latter approach, i.e. plasma emission spectroscopy, represents an indirect and rather qualitative measurement of oxygen vacancies in contrast to the established detection of UV absorption [11], photoluminescence [11–13] and other methods, e.g. the measurement of laser induced photocurrent [14]. However, the applied in situ plasma diagnostics stands out due to its high potential in time-critical applications, especially for real-time and inline measurements and process monitoring on industrial scale.

2 Basic considerations

Synthetic amorphous quartz glass, so-called fused silica, has established as one of the most important materials in optics, photonics and electronics. In contrast to the idealised description, fused silica does not purely consist of silicon dioxide (SiO_2) with a network given by perfect SiO_4 tetrahedrons where each oxygen atom appertains to two silicon (Si) atoms. In reality, further tetrahedrons of different chemical composition (Si_xO_y, where $0 \leq y \leq 4$) can occur in silicon oxide networks. Systems of that kind are referred to as silicon suboxide (SiO_x). Four different models currently describe the distribution of the involved tetrahedrons within this substoichiometric phase: according to the random bonding model (RBM) as suggested by Philipp, silicon suboxide consists of randomly composed and binominally distributed Si_xO_y tetrahedrons [15]. The random mixture model (RMM) as introduced by Temkin describes silicon suboxide as a mixed phase made up of clearly separated and homogeneous clusters of silicon (Si) and SiO_2 [16]. Another model, the matrix model (MM) was suggested by Hinds et al. assuming silicon suboxide to be given by clusters of Si embedded in a matrix of SiO_2 or clusters of SiO_2 embedded in a matrix of Si, respectively [17]. The interface cluster mixture model (ICMM) was presented by Hohl et al. and represents a combination of both the RBM and the RMM. According to this model, homogeneous Si and SiO_2 clusters are embedded into (and thus separated by) a boundary layer consisting of silicon suboxide and silicon monoxide [18].

Those four models thus indirectly describe the deficiency or vacancy of oxygen within silicon oxygen networks. In practice, such oxygen vacancy and further accompanying defects can be induced by chemical reduction and the mechanism of hydrolytic scission, i.e. the hydrogen-induced formation of fractures within SiO_2 networks. This mechanism is a well-known and common effect in glass melting where a certain amount of hydrogen ions (H^+) is provided by the ambient atmosphere and water vapour inside the melting furnace [19]. In this case, bridging oxygen is attacked by hydrogen ions, resulting in an intermediate,

$$\equiv \mathrm{Si} - \mathrm{O} - \mathrm{Si} \equiv + \mathrm{H}^+ \leftrightarrow (\equiv \mathrm{Si} - \mathrm{OH} - \mathrm{Si} \equiv)^+, \quad (1)$$

and a subsequent hydrolysis of this intermediate according to

$$(\equiv \mathrm{Si} - \mathrm{OH} - \mathrm{Si} \equiv)^+ + \mathrm{H_2O} \leftrightarrow 2(\equiv \mathrm{Si} - \mathrm{OH}) + \mathrm{H}^+. \quad (2)$$

In solid glasses, gamma irradiation can induce further hydrogen-related defects [20] where the defect formation is based on a reaction of SiO_2 and molecular hydrogen, H_2, according to

$$\equiv \mathrm{Si} - \mathrm{O} - \mathrm{Si} \equiv + \mathrm{H_2} \leftrightarrow \equiv \mathrm{Si} - \mathrm{OH} \quad \mathrm{H} - \mathrm{Si} \equiv . \quad (3)$$

As a result, both hydrogen and hydroxyl groups are implanted into the glass bulk material as shown by Boksay and Bouquet [21] and Charles [22, 23]. In addition to the formation of oxygen vacancies, given by several different types of oxygen deficiency centres (ODC), silicon oxide networks can thus feature a number of further defects. This involves the above-described implantation of hydrogen and the accompanying formation of H(I) centres and the formation of so-called E′ centres, i.e. generally speaking an unpaired free electron of a silicon atom as listed in Table 1.

It can be seen that the oxygen deficiency-related defects listed here are optically active and feature considerable absorption in the ultraviolet wavelength range, roughly between 160 and 400 nm. Apart from different mechanisms as for example irradiation with ultraviolet light [2] or gamma irradiation [13] such defects can also be induced by the use of chemically reductive plasmas. This approach was applied in the present work.

Table 1 Selection of optically active defects such as oxygen deficiency centres (ODC) in silicon dioxide related to oxygen deficiency including the corresponding absorption peaks (table adapted from [3])

Defect acronym	Absorption peak in nm	References
Oxygen deficiency centres I (ODC I)	163.14	[24–30]
E′—(surface)	196.80–206.64	[31]
ODC II—oxygen vacancy	177.12–182.33	[27, 32]
ODC II—oxygen divacancy	229.60–243.11	[33]
ODC II—dicoordinated silicon	393.60	[34]
E′-centres (bulk)	213.77–217.52	[35–37]
H(I)-centres	206.64–258.30	[38–40]

3 Experimental setup and experimentation

In this work, experiments were performed on commercially available drawn glass plates made of synthetic and amorphous fused silica. The samples were plasma-treated in a homemade plasma generator. This generator consists of a plasma source given by two opposite electrodes with an electrode distance, i.e. a discharge gap of 120 mm. The source was driven by a direct current (DC) electrical power supply. It was operated at three different voltages U and corresponding currents I, resulting in three different powers P dissipated in the plasma as calculated by the product of the voltage and the current ($P = U \cdot I$) and listed in Table 2.

The actual plasma generator is embedded in a cylindrical vacuum chamber made of stainless steel equipped with a pump periphery for low-pressure or vacuum generation. In order to initiate a chemical reduction of the glass-forming silicon dioxides, pure hydrogen was used as process gas where the gas pressure within the chamber was kept constant at 70 Pa during plasma treatment.

In the course of the treatment, the composition of the plasma within the chamber was measured via emission spectroscopy using an UV/VIS-spectrometer (USB 2000 from Ocean Optics, Inc.). Emission spectra were taken at the beginning of the plasma treatment process (i.e., the reference spectrum) and in steps of 10 min up to an overall treatment duration of 30 min where special attention was paid to the detected emission peaks related to oxygen and hydrogen. In addition to such plasma diagnostics, the transmission of the samples was measured prior to and after plasma treatment using a further UV/VIS-spectrometer (Lambda 1050 from PerkinElmer, Inc.) in order to verify the formation of oxygen deficiencies leading to an increase in UV absorption.

Table 2 Voltage and current applied for plasma treatment of fused silica including the accompanying power dissipated in the plasma

Voltage U in V	Current I in A	Dissipated power P in W
320	0.012	3.84
420	0.024	10.08
520	0.037	19.24

4 Results and discussion

4.1 Transmission

As shown in Fig. 1, the plasma treatment as described above leads to a decrease in transmission, corresponding to an increase in absorption of the treated fused silica samples. This behaviour can generally be observed for all applied plasma powers but turns out to be most significant in the case of the lowest power, i.e. 3.84 W.

Such effect of plasma-induced decrease in transmission due to the application of hydrogenous plasma is generally well known and was already reported in previous work [9, 10]. However, the observed impact of plasma power on this process has not yet been extensively investigated and is thus discussed in more detail in Sect. 4.2. The observed decrease in transmission is preferably found in the UV wavelength range, i.e. from the lowest measured wavelength, 200 nm, up to approximately 400 nm. It can thus be attributed to a plasma-induced and hydrogen-driven formation of optically active defects as introduced in Sect. 2, namely oxygen (di)

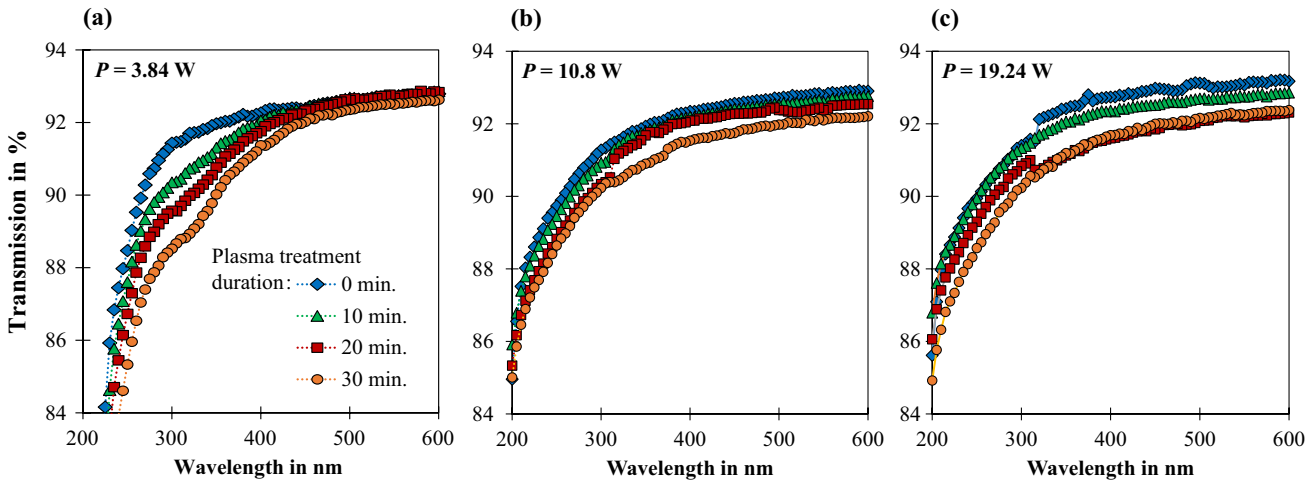

Fig. 1 Impact of plasma treatment at different plasma powers on the spectral transmission of fused silica samples

vacancies, H(I) centres and E′-bulk centres, within the fused silica bulk material [3].

This mechanism is also visualised by the time-dependent change in transmission of the particular absorption peaks or peak ranges of these defects as shown in Fig. 2. It can be seen that transmission continuously decreases with increasing plasma treatment duration.

All the three defects considered in Fig. 2 result from the removal of oxygen from the glass network. As an example, this can be initiated by neutral hydrogen, which occurs within the plasma due to electron-impact dissociation of H_2 molecules according to

$$SiO_2 + 2H \leftrightarrow SiO + H_2O \quad (4)$$

where volatile gaseous water is formed as a by-product. At the same time hydrogen is implanted and attached to oxygen deficiency centres, finally forming H(I) centres. Such plasma-induced implantation of hydrogen as well as the chemical reduction and the accompanying decrease in oxygen content in the near-surface glass material is described in more detail in [9, 41] where both effects were verified via secondary ion mass spectroscopic (SIMS) measurements on plasma-treated fused silica. In the present work, the removal of oxygen from the glass network was indirectly detected by measuring the composition of the plasma as discussed in more detail in the following section.

4.2 Plasma diagnostics

The use of a low-pressure plasma discharge within a housed vacuum chamber allows an easy and reliable analysis of the composition of the plasma via emission spectroscopy since any impact of the surrounding medium, air, on the measured signal is obviated. As shown by the difference spectrum in Fig. 3, an obvious increase in intensity of six different discrete emission lines can be observed in the course of the plasma treatment process. The presented difference spectrum was calculated from the emission spectra detected at the end ($t_{max} = 30$ min) and the beginning ($t_0 = 0$ min) of a plasma treatment process at a power of 3.84 W. It thus visualises the change in plasma composition that occurred in a period of 30 min, i.e. the overall treatment time.

All of the increased emission lines in Fig. 3 can be attributed to oxygen. The five observed lines at 366.25 nm, 376.25 nm, 486.49 nm, 648.39 nm and 657.11 nm relate to different transitions of singly ionised oxygen, OII [42]. Moreover, the line with the most significant change at 745.54 nm corresponds to doubly ionised oxygen, OIII [43]. When taking a closer look on the time-dependency of the particular line intensities, it further turns out that the amount

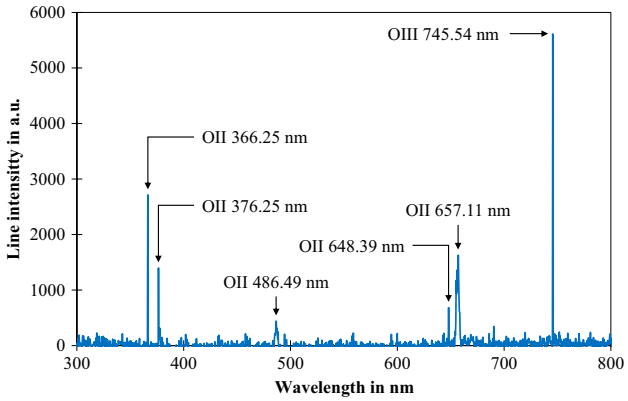

Fig. 3 Difference spectrum of the plasma (at $t_{max} = 30$ min–$t_0 = 0$ min) at a plasma power of 3.84 W

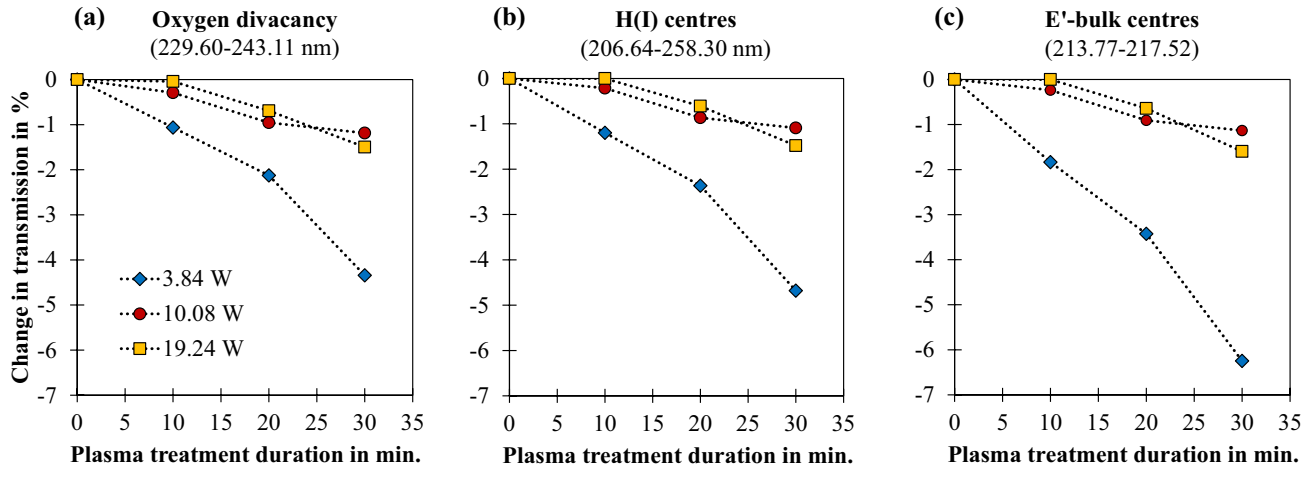

Fig. 2 Plasma power-dependent change in transmission for three different wavelength ranges, representing oxygen divacancy (**a**), H(I) centres (**b**) and E′ bulk centres (**c**) versus plasma treatment duration

of oxygen within the chamber is continuously increasing in the course of the plasma treatment; see Fig. 4.

This increase is inversely proportional to the decrease in transmission shown in Fig. 2 and thus indicates a release of oxygen from the fused silica network and the accompanying formation of oxygen (di)vacancies by the hydrogenous plasma, for example, according to Eq. (4), and an additional implantation of hydrogen into the glass. It further turns out that the observed increase in line intensity as well as the above-presented decrease in transmission is strongly dependent on plasma power: The higher the power, the lower the process efficiency in terms of inducing optically active defects related to oxygen deficiencies. This point is of particular interest for a potential application of plasma-induced increase in absorption, for example, for subsequent laser processing of transparent media.

There are different approaches for explaining the decrease in plasma process efficiency with increasing plasma power [44]. For instance, increasing the plasma power may result in a decrease in available plasma species required for initiating the formation of oxygen deficiency centres in glass. Apparently, one important species is atomic hydrogen that is formed in the plasma due to electron-impact-based dissociation of the working gas, molecular hydrogen. According to Eq. (4) and due to its extremely high chemical reactivity [45], such atomic hydrogen could form volatile, gaseous water after reacting with oxygen from silicon dioxide. The water molecule is based on a covalent binding, a.k.a. atomic bond; the involved atoms, i.e. hydrogen and water, thus share the electrons. The formation of this type of bond could be hindered when increasing the plasma power since as a result, the plasma's degree of ionisation is increased as well. Consequently, the amount of the required atomic (and electrically neutral, i.e. neither excited nor ionised) hydrogen within the plasma volume is reduced.

This assumption is supported by the emission spectroscopic measurements performed in the present work. As shown in Fig. 5, an increase in plasma power comes along with an increase in line intensity of characteristic Balmer lines, namely Hα (656.45 nm), Hβ (486.14 nm), Hγ (434.05 nm) and Hδ (410.17 nm), corresponding to an increased emission of photons by electrons in excited states.

It can thus be stated that increasing the plasma power directly leads to an increase in excited—and thus light-emitting—hydrogen atoms. Since the total amount of hydrogen atoms was kept constant as managed via the constant process pressure of 70 Pa, the number of available neutral hydrogen atoms is consequently decreased when increasing the plasma power.

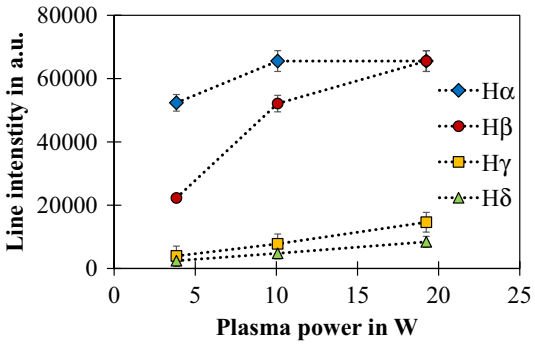

Fig. 5 Line intensity of the first four Balmer lines of electron transition in hydrogen atoms at a plasma treatment duration of 30 min versus plasma power

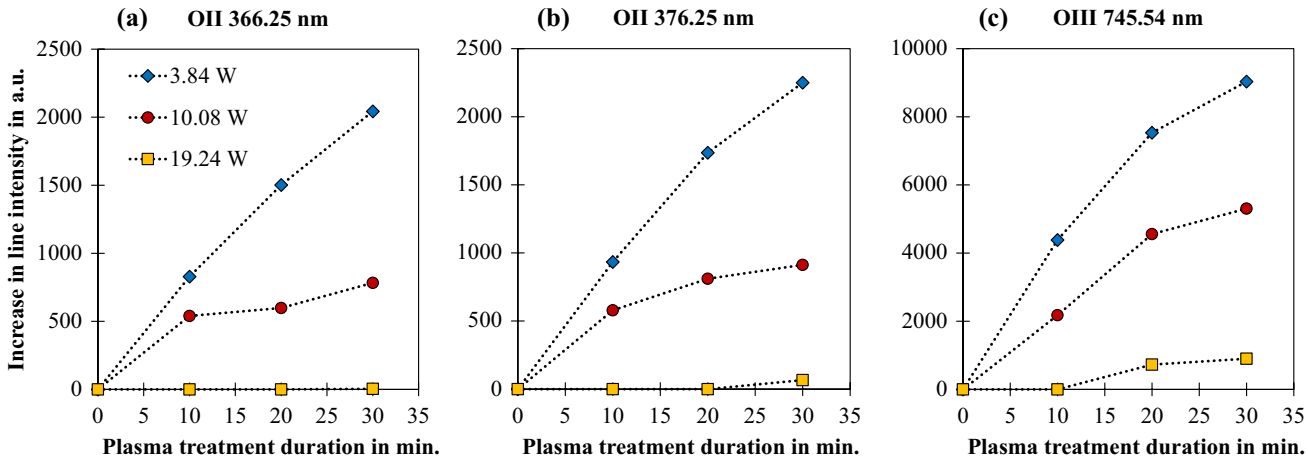

Fig. 4 Increase in line intensity of three selected emission lines of oxygen at 366.25 nm (**a**), 376.25 nm (**b**) and 745.54 nm (**c**) of the plasma versus plasma treatment duration. Please note the different scalings of the *y* axes

5 Conclusions

The presented results show that the applied plasma affects the chemical composition and thus the optical properties of silicon dioxide-based glass surfaces. This fact might be of interest for the development of novel plasma-based techniques as for example a controlled refraction index matching prior to or during coating processes. It is also of practical interest for existing plasma methods for glass or silicon dioxide treatment using hydrogenous process gases, e.g. cleaning [46, 47] or chemical vapour deposition [48, 49]. In the latter case, discrepancies between a theoretical, calculated layer design and the actual, real properties could be due to an alteration of the glass substrate during the coating process. The indirect inline monitoring of the formation of glass defects via the observation of the plasma as suggested in the present work could allow for a reduction of such discrepancies and the accompanying improvement of high precision coatings. The approach of plasma diagnostic could further be enhanced by an additional application of infrared spectroscopy for the detection of molecules such as gaseous water. Since this action would significantly improve inline detection processes, it will be investigated in future work. Another work to be performed is a further decrease in plasma power in order to identify the optimum plasma parameters for the target application, i.e. defect formation in fused silica.

Acknowledgements Open Access funding provided by Projekt DEAL. The authors thank the Institut Universitaire de Technologie A de Lille and the Technische Hochschule Wildau for realising the staff exchange that led to the results presented in this contribution.

Author contributions CG and MH contributed to the conception and design of the presented study and supervised the experimental part. EL and TC performed material preparation, experimentation, data collection and first analysis. CG carried out final analysis and wrote the first draft of the manuscript. All authors reviewed and approved the final manuscript.

Open Access This article is licensed under a Creative Commons Attribution 4.0 International License, which permits use, sharing, adaptation, distribution and reproduction in any medium or format, as long as you give appropriate credit to the original author(s) and the source, provide a link to the Creative Commons licence, and indicate if changes were made. The images or other third party material in this article are included in the article's Creative Commons licence, unless indicated otherwise in a credit line to the material. If material is not included in the article's Creative Commons licence and your intended use is not permitted by statutory regulation or exceeds the permitted use, you will need to obtain permission directly from the copyright holder. To view a copy of this licence, visit http://creativecommons.org/licenses/by/4.0/.

References

1. V.K. Tikhomirov, A.B. Seddon, D. Furniss, M. Ferrari, J. Noncryst. Solids **326–327**, 296 (2003)
2. M. Essid, J. Albert, J.L. Brebner, K. Awazu, J. Noncryst. Solids **246**, 39 (1999)
3. L. Skuja, J. Noncryst. Solids **239**, 16 (1998)
4. J. Qiu, A.L. Gaeta, K. Hirao, Chem. Phys. Lett. **333**, 236 (2001)
5. T. Uchino, M. Takahashi, T. Yoko, Phys. Rev. B **62**, 2983 (2000)
6. J. Hoffmeister, C. Gerhard, S. Brückner, J. Ihlemann, S. Wieneke, W. Viöl, Phys. Proc. **39**, 613 (2012)
7. S. Brückner, J. Hoffmeister, J. Ihlemann, C. Gerhard, S. Wieneke, W. Viöl, J. Laser Micro Nanoeng. **7**, 73 (2012)
8. C. Gerhard, M. Dammann, S. Wieneke, W. Viöl, Micromachines **5**, 408 (2014)
9. C. Gerhard, D. Tasche, S. Brückner, S. Wieneke, W. Viöl, Opt. Lett. **37**, 566 (2012)
10. C. Gerhard, T. Weihs, D. Tasche, S. Brückner, S. Wieneke, W. Viöl, Plasma Chem. Plasma Process. **33**, 895 (2013)
11. S. Munekuni, T. Yamanaka, Y. Shimogaichi, R. Tohmon, Y. Ohki, K. Nagasawa, Y. Hama, J. Appl. Phys. **68**, 1212 (1990)
12. Y. Sakurai, K. Nagasawa, H. Nishikawa, Y. Ohki, J. Appl. Phys. **86**, 370 (1999)
13. Y. Sakurai, J. Noncryst. Solids **352**, 5391 (2006)
14. V.N. Bagratashvili, S.I. Tsypina, P.V. Chernov, A.O. Rybaltovskii, Y.S. Zavorotny, S.S. Alimpiev, Y.O. Simanovskii, L. Dong, P.S.J. Russel, Appl. Phys. Lett. **68**, 1616 (1996)
15. H.R. Philipp, J. Phys. Chem. Solids **32**, 1935 (1971)
16. R.J. Temkin, J. Noncryst. Solids **17**, 215 (1975)
17. B.J. Hinds, F. Wang, D.M. Wolfe, C.L. Hinkle, G. Lucovsky, J. Vac. Sci. Technol. B **16**, 2171 (1998)
18. A. Hohl, T. Wieder, P.A. van Aken, T.E. Weirich, G. Denninger, M. Vidal, S. Oswald, C. Deneke, J. Mayer, H. Fuess, J. Noncryst. Solids **320**, 255 (2003)
19. L.R. Pederson, Phys. Chem. Glasses **28**, 17 (1987)
20. H. Nishikawa, R. Tohmon, Y. Ohki, K. Nagasawa, Y. Hama, J. Appl. Phys. **65**, 4672 (1989)
21. Z. Boksay, G. Bouquet, Phys. Chem. Glasses **21**, 110 (1980)
22. R.J. Charles, J. Appl. Phys. **29**, 1549 (1958)
23. R.J. Charles, J. Appl. Phys. **29**, 1554 (1958)
24. M. Guzzi, F. Pio, G. Spinolo, A. Vedda, C.B. Azzoni, A. Paleari, J. Phys.: Condens. Mater **4**, 8635 (1992)
25. M. Guzzi, M. Martini, A. Paleari, F. Pio, A. Vedda, C.B. Azzoni, J. Phys.: Condens. Mater **5**, 8105 (1993)
26. H. Nishikawa, R. Nakamura, Y. Ohki, Y. Hama, Phys. Rev. B **48**, 15584 (1993)
27. H. Nishikawa, E. Watanabe, D. Ito, Y. Ohki, Phys. Rev. Lett. **72**(2101), 2101 (1994)
28. H. Imai, K. Arai, H. Imagawa, H. Hosono, Y. Abe, Phys. Rev. B **38**, 12772 (1988)
29. H. Hosono, Y. Abe, H. Imagawa, H. Imai, K. Arai, Phys. Rev. B **44**, 12043 (1991)
30. S. Hayashi, K. Awazu, H. Kawazoe, J. Noncryst. Solids **179**, 235 (1994)
31. A.A. Bobyshev, V.A. Radtsig, Kinet. Katal. **29**, 638 (1988)
32. E.P. O'Reilly, J. Robertson, Phys. Rev. B **27**, 3780 (1983)
33. L.N. Skuja, A.N. Streletsky, A.B. Pakovich, Solid State Commun. **50**, 1069 (1984)
34. L. Skuja, J. Noncryst. Solids **179**, 51 (1994)
35. D.L. Griscom, Nucl. Instrum. Methods B **1**, 481 (1984)
36. R. Boscaino, M. Cannas, F.M. Gelardi, M. Leone, Nucl. Instrum. Methods B **116**, 373 (1996)
37. H. Nishikawa, E. Watanabe, D. Ito, Y. Ohki, J. Noncryst. Solids **179**, 179 (1994)

38. V.A. Radtsig, A.A. Bobyshev, Phys. Status Solidi B **133**, 621 (1986)
39. T. Tsai, D.L. Griscom, J. Noncryst. Solids **91**, 170 (1987)
40. V.A. Radzig, V.N. Bagratashvili, S.I. Tsypina, P.V. Chernov, A.O. Rybaltovskii, J. Phys. Chem. **99**, 6640 (1995)
41. D. Tasche, C. Gerhard, J. Ihlemann, S. Wieneke, W. Viöl, J. Eur. Opt. Soc. Rapid **9**, 14026 (2014)
42. I. Wenåker, Phys. Scr. **42**, 667 (1990)
43. D. Luo, A.K. Pradhan, H.E. Saraph, P.J. Storey, Y. Yu, J. Phys. B At. Mol. Opt. **22**, 389 (1989)
44. C. Gerhard, E. Letien, T. Cressent, M. Hofmann, Wiss. Beitr. **23**, 33 (2019)
45. H. Shirai, Y. Fujimura, S. Jung, Thin Solid Films **407**, 12 (2002)
46. V. Gupta, N. Madaan, D.S. Jensen, S.C. Kunzler, M.R. Linford, Langmuir **29**, 3604 (2013)
47. Y.-B. Park, S.-W. Rhee, Appl. Phys. Lett. **68**, 2219 (1996)
48. C.M.T. Hodson, J. Wood, M. Middleton, Proc. ESSDERC **87**, 229 (1987)
49. G. Kelm, G. Jungnickel, Mat. Sci. Eng. A Struct. **139**, 401 (1991)

Publisher's Note Springer Nature remains neutral with regard to jurisdictional claims in published maps and institutional affiliations.